^{1}H NMR Study of the Base-Pairing Reactions of d(GGAATTCC): Salt and Polyamine Effects on the Imino Proton Exchange†

William H. Braunlin‡ and Victor A. Bloomfield*

Department of Biochemistry, The University of Minnesota, St. Paul, Minnesota 55108

Received July 6, 1987; Revised Manuscript Received October 21, 1987

ABSTRACT: Salts and polyamines have a variety of effects on the physical properties of DNA, including stabilization against thermal melting. We wished to gain greater insight into the mechanism of this stabilization by ascertaining its effect on the dynamics of base opening and closing reactions, as measured by NMR. Since the binding of spermidine(3+) is influenced by salt, and since spermidine may act as a base catalyst in proton exchange reactions, we have undertaken a study of salt and base catalyst effects on the imino proton exchange kinetics of a model oligomeric DNA. The selective longitudinal NMR relaxation rates of the hydrogen-bonded imino protons of the self-complementary octadeoxyribonucleotide d(GGAATTCC) monitor the rate of the base-catalyzed chemical exchange of these protons with solvent water. The exchange rates thus obtained provide a sensitive measure of the base-pair opening reactions of the DNA duplex. Under conditions of low pH and no added base catalyst, the NMR relaxation rates allow the determination of k_d, the rate constant for the dissociation of the octameric duplex into single strands. Titration with the base catalyst tris(hydroxymethyl)aminomethane allows the determination of k_{op}, the rate constant for the localized opening of individual base pairs, prior to dissociation. A significant Na^+ concentration dependence is found for k_d. From an analysis of this dependence, it is determined that 0.6 ± 0.1 sodium ion is released during the dissociation event. The activation energy for helix dissociation (200 ± 5 kJ/mol) is not dependent on the sodium ion concentration, indicating that the dissociation is entropically driven by the release of bound sodium ions. In agreement with previous results, no measurable salt dependence is found for k_{op}, which is equal to about 100 s^{-1} at 25 °C. Under low-salt conditions, the trivalent cation spermidine decreases the rate of helix dissociation, again without affecting the activation energy for this process. Diprotonated spermidine(2+) acts as an extremely effective catalyst of imino proton exchange.

Our current understanding of the details of DNA conformation, dynamics, and interactions with proteins and small molecules has grown in concert with the development of an efficient technology for producing milligram quantities of highly pure, defined-sequence oligodeoxynucleotides. Because individual proton resonances may be studied, and since cross-relaxation effects are much less pronounced than in polymeric DNA, NMR studies of oligonucleotides have provided much previously inaccessible information concerning the solution structure and dynamics of double-helical DNA (Patel et al., 1982c; Kearns, 1984; Wemmer & Reid, 1985).

Ions have many important effects on the behavior of nucleic acids. Simple salts raise the thermal melting temperature of double-helical DNA and affect the binding of ligands (Record et al., 1981). Polyamines such as spermidine and spermine have these general effects (Bloomfield & Wilson, 1981) and also influence the conformation of nucleic acids, inducing bending of double-helical regions of tRNA (Quigley et al., 1978), transition to the left-handed Z form of DNA (Rich et al., 1984; Behe & Felsenfeld, 1981), and condensation of DNA into compact toroidal structures (Gosule & Schellman, 1976; Wilson & Bloomfield, 1979). In an attempt to understand how these effects may be produced at the molecular level, we have undertaken an investigation by NMR of salt and spermidine effects on the base-pairing dynamics of oligomeric DNA.

The NMR behavior of the octameric duplex d(GGAATTCC) has previously been characterized over a limited range of solution conditions (Patel & Canuel, 1979; Connolly & Eckstein, 1984; Broido et al., 1984, 1985). Proton resonances have been assigned (Broido et al., 1984, 1985), as have all seven ^{31}P resonances (Connolly & Eckstein, 1984). Differential scanning calorimetry measurements have been performed on this molecule, and the results obtained are well described by a two-state model for the helix–coil transition (Patel et al., 1982b). Because of this thorough initial characterization of the NMR and helix–coil equilibrium behaviors of this molecule, we felt that it would be a good subject for a more detailed NMR study of the salt and polyamine dependences of its base-pairing equilibria and kinetics.

d(GGAATTCC) is of further interest since it contains the recognition site for the *Eco*RI restriction enzyme. A dodecamer, d(CGCGAATTCGCG), possessing this site provided the first B-DNA crystal structure determined, as well as the first crystal structure of a protein–DNA complex (Dickerson & Drew, 1981; Grable et al., 1984). This dodecamer has also been well studied by NMR, and not surprisingly, the internal resonances show some homology to the corresponding resonances on the octamer (Patel et al., 1982a).

The nuclear magnetic relaxation of the imino protons involved in the Watson–Crick base pairs of double-helical DNA is sensitive to the rate of exchange of these protons with solvent water. Under appropriate conditions, this exchange rate in turn provides a measure of the kinetics of base-pairing opening (Crothers et al., 1974; Johnston & Redfield, 1981). In the present paper, we present the results of our NMR measurements on these protons to determine rate constants for the salt

† Supported by NIH Grant GM28093.

* Correspondence should be addressed to this author.

‡ Present address: Department of Chemistry, Polytechnic University, 333 Jay St., Brooklyn, NY 11201.

0006-2960/88/0427-1184$01.50/0

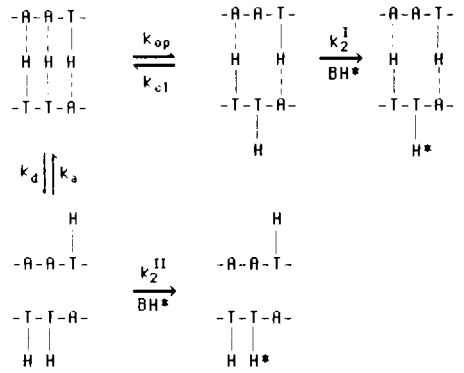

FIGURE 1: Kinetic model illustrating the two imino proton exchange pathways for GGAATTCC. The upper pathway (pathway I) represents exchange following a small-scale opening of one or a few base pairs of the duplex. The lower pathway (pathway II) represents exchange following complete dissociation of the duplex into single strands.

and polyamine-dependent base-pair opening kinetics of d(GGAATTCC). In a later paper (W. H. Braunlin and V. A. Bloomfield, unpublished results), we will combine these results with the results of chemical shift and line-width measurements of the nonexchangeable base proton resonances to provide a more complete characterization of the salt dependence of the helix–coil equilibria and kinetics of this molecule.

THEORY

As described under Methods, selective spin–lattice relaxation rates ($R_{1,sel}$) may be measured by the inversion–recovery method by applying long, low-power 180° radio-frequency pulses centered on the NMR resonance of interest, followed by nonselective 90° pulses. $R_{1,sel}$ of the imino proton resonances of oligomeric DNA contains contributions from the base-catalyzed chemical exchange of these protons with solvent water. Under the conditions of our experiments, this relaxation is governed by the simple equation:

$$R_{1,sel} = R_{1,M} + k_{ex} \quad (1)$$

where $R_{1,M}$ represents contributions from dipolar–dipolar magnetic interactions and k_{ex} is the rate of chemical exchange of the imino proton with water. By analyzing our data according to eq 1, we are ignoring the potentially different relaxation rates of the closed and open states. This procedure is justified since under the conditions of our experiments the imino protoins examined spend a negligibly small fraction of time in the open state (Bendel, 1987).

In Figure 1, we present a kinetic model illustrating the two different pathways of imino proton exchange for oligomeric duplexes (Pardi & Tinoco, 1982). Exchange may occur either following small-scale opening of individual base pairs (pathway I) or following dissociation of the duplex into two single strands (pathway II). Exchange of an *exposed* imino proton (AH) occurs through formation of a hydrogen-bonded intermediate with base catalyst B (Eigen, 1964; Leroy et al., 1985):

$$AH + B \rightleftarrows [AH\text{–}B] \rightleftarrows A^- + BH^+ \quad (2)$$

The fraction of encounters between AH and B that result in proton exchange is given by $1/(1 + 10^{-\Delta pK})$, where $\Delta pK = pK_B - pK_A$. The rate of proton transfer, $k_{tr} = k_2[B]$, is then given by

$$k_{tr} = k_D/(1 + 10^{-\Delta pK}) \quad (3)$$

where k_D is the collision rate of A with B. If k_R is the diffusion-limited association rate constant (usually around 10^{10} M^{-1} s^{-1}), then, following Leroy et al. (1985), we define an "accessibility" factor α ($0 < \alpha \leq 1$).

Referring again to Figure 1, we may write for the general case:

$$k_{ex} = k_{op}k_{tr}^{I}/(k_{tr}^{I} + k_{cl}) + k_d k_{tr}^{II}/(k_{tr}^{II} + k_a C_t) \quad (4)$$

where C_t is the total strand concentration of oligomer. As we argue below, under the conditions of our experiments, we always have $k_{tr}^{II} \gg k_a C_t$ (that is, proton exchange from the strand-dissociated state is much faster than strand reassociation), and may thus rewrite eq 4 as

$$k_{ex} = k_{op}k_{tr}/(k_{tr} + k_{cl}) + k_d \quad (5)$$

where we have for convenience left the superscript off of k_{tr}^{I}.

We consider the following two limiting cases: (1) Under conditions of low added base catalyst and low pH, we have $k_{cl} \gg k_{tr}$. Relaxation occurs mainly by pathway II, and eq 1 holds with $k_{ex} = k_d$. (2) For high added catalyst and high pH, a situation is approached where $k_{tr} \gg k_{cl}$. Pathway I now dominates the relaxation, and eq 1 holds with $k_{ex} = k_{op}$.

A transition region between these two extremes is also of interest. At intermediate concentrations of base catalyst, k_{cl} is of the same order of magnitude as k_{tr}. Under these conditions, we may utilize the analysis of Leroy et al. (1985) for imino proton exchange from polynucleotide helices. Substituting $\tau_{ex} = (k_{ex} - k_d)^{-1}$, $\tau_0 = k_{op}^{-1}$, and $B_{eq} = k_{cl}[B]/k_{tr}$ (B_{eq} is the concentration for which $k_{cl} = k_{tr}$), eq 5 may be rearranged as

$$\tau_{ex} = \tau_0(1 + B_{eq}/[B]) \quad (6)$$

and the limiting slope of a plot of $\tau_{ex} = (R_{1,sel} - R_{1,M} - k_d)^{-1}$ vs. $1/B$ will give τ_0 as the y intercept and B_{eq} from the slope. Combining eq 6 with eq 3 and using the relation $k_D = \alpha k_R[B]$ result in

$$\frac{k_{cl}}{\alpha} = \frac{k_R B_{eq}}{1 + 10^{-\Delta pK}} \quad (7)$$

In the application of this equation to determine values for k_{cl}/α, the diffusion-limited value of 10^{10} M^{-1} s^{-1} will be assumed for k_R.

As we demonstrate below, by varying the pH and base catalyst concentrations, we are able to obtain salt- and polyamine-dependent kinetic parameters for the opening events of each of the two pathways of Figure 1.

MATERIALS AND METHODS

Materials. d(GGAATTCC) was synthesized on a silica gel support by the phosphite triester method (Narang et al., 1979, 1980) using a SYSTEK automated DNA synthesizer. A typical round of synthesis gave 2–3 mg of octamer. By pooling samples from three to four such rounds, we were able to obtain enough DNA for our NMR experiments. Following synthesis, the oligomer was cleaved from the support by soaking in concentrated NH_4OH for 3 h at room temperature. Protecting benzyl and isobutyl groups were subsequently removed by heating the NH_4OH solution for 12 h at 50–55 °C. NH_4OH was then removed by evaporation, leaving a white powder which was dissolved in H_2O and extracted twice with butanol. The aqueous solution was dialyzed several hours against two changes of buffer containing 10 mM NaCl, 1 mM sodium cacodylate, and 0.1 mM ethylenediaminetetraacetic acid (EDTA), pH 6.5. All dialyses were performed by using Spectrapor cellulose tubing with a molecular weight cutoff of 1000. Proton NMR of the samples thus prepared showed no indication of organic contaminating materials.

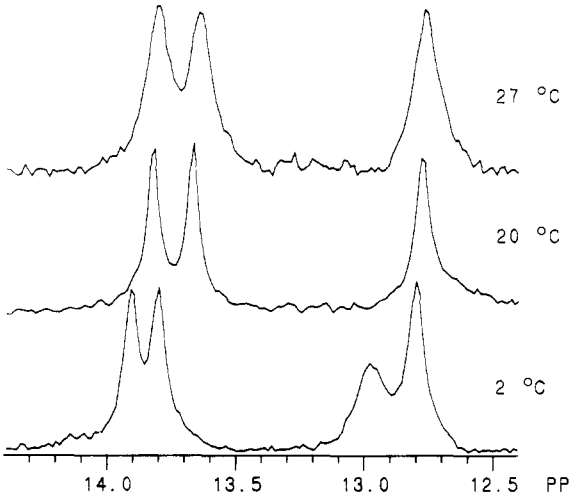

FIGURE 2: Temperature dependence of the imino proton region of the ^{1}H NMR spectrum of GGAATTCC. The spectra were recorded for a sample containing 14.4 mM DNA octamer strand, 0.1 M Na^+, and 1 mM EDTA, pH 6.5.

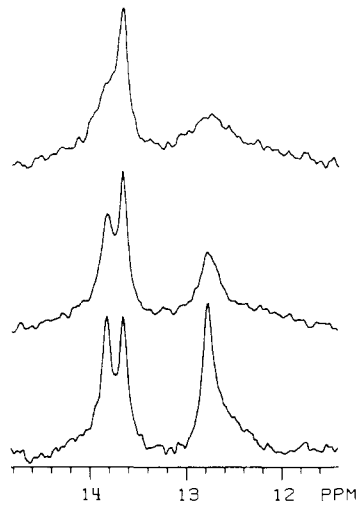

FIGURE 3: pH dependence at 25 °C of the imino proton region for a sample containing 0.075 M Na^+, 11.5 mM GGAATTCC strand, and 1 mM EDTA. The pH was monitored with a microelectrode over the course of a titration with HCl. The upper spectrum corresponds to pH 8.6, the middle to pH 7.8, and the lower to pH 6.1.

Methods. GGAATTCC strand concentrations were obtained by using $\epsilon_{260} = 5.4 \times 10^4$ M^{-1} cm^{-1} (Patel & Canuel, 1979). Sodium ion concentrations for all stock GGAATTCC solutions were determined by inductively coupled plasma spectroscopy, performed by the Analytical Services Laboratory of The University of Minnesota. Titrations were performed by adding microliter amounts of concentrated stock solutions directly to 5-mm microtubes (Wilmad 508CP) containing a total volume of 0.13–0.15 mL of DNA solution. pH was determined either at high pH by measuring with a combination microelectrode or at low pH by monitoring the chemical shift of the cacodylate methyl resonance (Valcour & Woodworth, 1986). Concentrations of the basic form of tris(hydroxymethyl)aminomethane (Tris) were determined by using a value of 8.14 for the pK_a of Tris at 25 °C (Good et al., 1966). The pK_a was taken to be 8.34 for the ionization equilibrium between spermidine(3+) and spermidine(2+) (Hedwig & Powell, 1973). The pK_a for the ionization of thymidine N3 was taken to be 9.79 (Ts'o, 1974).

NMR measurements of the exchangeable imino protons were performed on a Nicolet 300-MHz spectrometer. Measurements were performed in H_2O solution containing 15% D_2O to allow locking on the deuterium signal. Water suppression was obtained by using the Redfield 214 low-power pulse sequence (Redfield et al., 1975). Selective spin–lattice relaxation rates were measured by the inversion–recovery method by applying a long (3.4 ms) 180° decoupler pulse centered on the signal of interest, followed by a nonselective 90° Redfield pulse, centered around 13 ppm. In this manner, better than 90% inversion was routinely obtained. Chemical shifts were determined relative to sodium 3-(trimethylsilyl)-1-propanesulfonate (DSS), $(CH_3)_3Si(CH_2)_3SO_3Na_2$, which was added to the samples as an internal standard.

RESULTS

Imino Proton Spectra. The numbering scheme that we shall use for the imino protons in the GGAATTCC duplex is the same as that employed by Patel and Canuel (1979). The four distinct imino proton resonances are numbered beginning at either end and moving toward the center (i.e., TH3 4 refers to the innermost imino resonance). Figure 2 shows temperature-dependent spectra of these protons, determined under low-pH conditions (pH 6.5). The two pairs of resonances are readily assigned according to type since thymine imino protons in A-T base pairs are known to resonate downfield of guanine imino protons in G-C base pairs (Patel & Canuel, 1979). On the basis of Figure 2, the terminal guanosine H-1 (GH1 1) proton is readily assigned since it is visible only at low temperatures. Above about 10 °C, this signal is broadened into the base line due to rapid opening and closing ("fraying") of the terminal base pair. The remaining three internal imino resonances broaden and disappear as a group as the temperature is raised (Patel & Canuel, 1979). The two remaining thymine imino protons may be tentatively assigned on the basis of the pH-dependent spectra shown in Figure 3. Since fraying is expected to be greatest toward the ends of the helix and to decrease toward the center, the sequential broadening with increasing pH of the resonances of Figure 3 allows the lowest field TH3 proton to be assigned to TH3 3 and the highest field proton to TH3 4. As shown in Figure 4, the NOEs observed between the TH3 imino resonances and the nonexchangeable AH2 resonances on the base-paired adenines are consistent with the tentative assignments of the AH2 resonances by Broido and colleagues (Broido et al., 1984, 1985). We note the close similarity between the TH3 shifts reported here and the shifts for the corresponding resonances on the CGCGAATTCGCG and GAATTCGCG duplexes (Patel et al., 1982a,b).

Imino Proton Relaxation at Low pH. Semiselective T_1 measurements of the relaxation of the thymine imino protons were performed by centering a long decoupler pulse at a frequency between the frequencies of the two thymine resonances. As is shown in Figure 5, better than 90% inversion is obtained for these resonances, without significant excitation of the nearby GH1 2 proton. Similarly, the GH1 2 proton may be selectively excited without affecting either the thymine imino protons or the aromatic base protons (7.2–8.2 ppm). As a consequence, it is clear that the imino proton resonances are magnetically isolated from the water resonance, as they must be for eq 1 to apply (Bendel, 1987). In Figure 6, an Arrhenius plot of the temperature dependence of $R_{1,sel}$ is shown for the three internal imino proton resonances under conditions of low pH (pH 6.5). Under these conditions, the three internal resonances show nearly identical temperature-dependent relaxation rates. If $R_{1,M}$ (eq 1) decreases as expected with the viscosity divided by temperature, then the low-temperature points (for which $R_{1,sel} = R_{1,M}$) may be extrapolated by using the known dependence of the viscosity of water on temperature

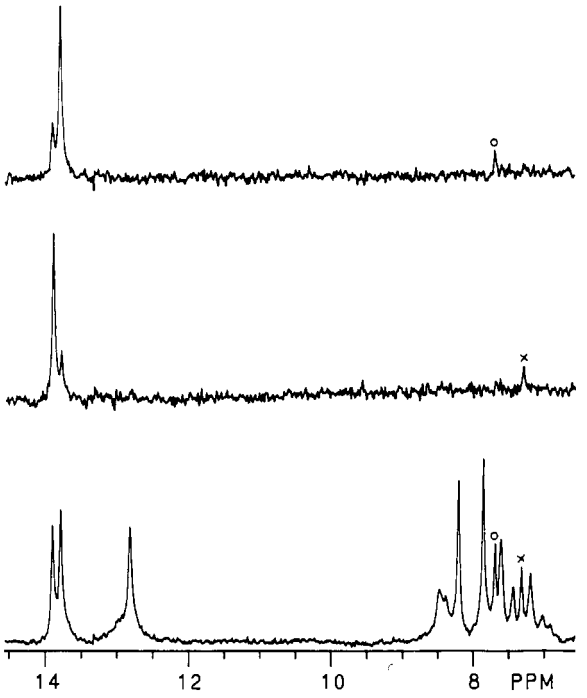

FIGURE 4: NOE measurements demonstrating the connectivity between the AH2 protons and the TH3 imino protons on GGAATTCC. The lower curve shows the imino and base proton regions of the 300-MHz proton spectrum of GGAATTCC in 85% H_2O/15% D_2O. The middle curve is a difference NOE spectrum showing that when the TH3 3 imino proton is saturated, the nonexchangeable AH2 3 proton exhibits a negative NOE. The upper curve shows that saturation of TH3 4 results in magnetization transfer to AH2 4. The sample contained 0.1 M Na^+, 14.4 mM DNA strand, and 1 mM EDTA, pH 6.5. The temperature was held constant at 10 °C.

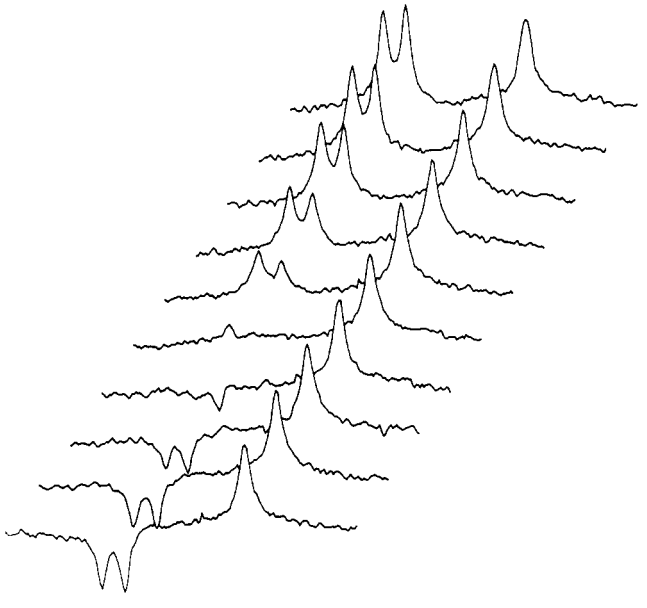

FIGURE 5: Imino proton spectra obtained for a semiselective inversion–recovery experiment at 26 °C for a sample containing 0.1 M Na^+, 14.4 mM DNA strand, and 1 mM EDTA, pH 6.5. A 3.4-ms decoupler pulse centered between the two TH3 imino resonances (13.7 ppm) was used to invert these resonances. Following a delay time ranging from 2 ms (bottom spectrum) to 80 ms (top spectrum), a 90° Redfield water suppression pulse was applied centered at 13.4 ppm. These spectra illustrate how we were able to selectively invert the TH3 imino resonances without significantly perturbing the GH2 imino resonances.

(Weast, 1983) to determine $R_{1,M}$ at higher temperature. Using eq 1, we are thus able to determine k_{ex} and E_a for the exchange of the internal imino protons with water. Figure 6 also shows

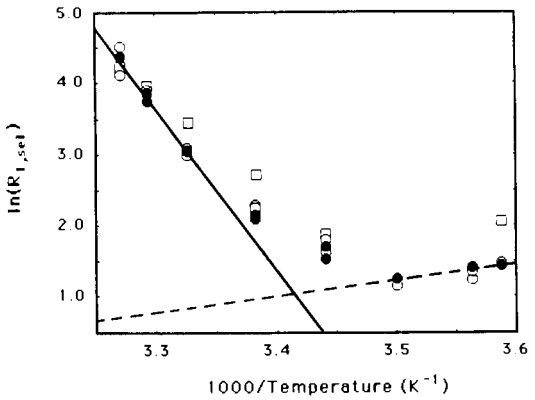

FIGURE 6: Arrhenius plot showing the temperature dependence of $R_{1,sel}$ for the three internal imino protons of GGAATTCC for a sample containing 0.19 M Na^+, 2.4 mM octamer strand, 0.3 mM EDTA, and 3 mM cacodylate, pH 6.0. Closed circles are data for TH3 4, open circles are for TH3 3, and open squares are for GH2 2. As described in the text, the low-temperature data were extrapolated by using the known temperature dependence of the viscosity of water to obtain the dashed line in the figure, which represents the temperature dependence of $R_{1,M}$, the magnetic contribution to $R_{1,sel}$. The solid line shows the best linear fit of ln ($R_{1,sel} - R_{1,M}$) vs the inverse of the temperature and represents the exchange contribution to $R_{1,sel}$. From this line, we obtain E_a = 170 (±10) kJ/mol and k_d = 22 ± 2 s^{-1} at 25 °C.

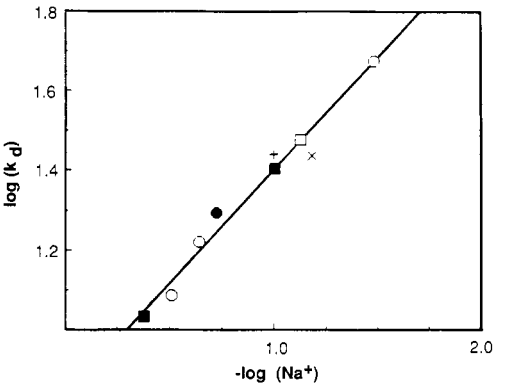

FIGURE 7: Dependence of the duplex dissociation rate constant k_d on sodium ion concentration: (■) 0.8–0.9 mM strand, (●) 2.4 mM strand; (○) 5–7 mM DNA strand; (×) 7.7 mM strand; (□) 11.5 mM strand; (+) 14.4 mM strand. k_d values were determined from $R_{1,sel}$ values measured at 25 °C for the TH3 4 resonance, using eq 1 with $R_{1,M}$ = 2.0 s^{-1}. The best linear least-squares fit to all points (solid line) gives log k_d = −0.57 (±0.1) log [Na^+] + 0.83 (±0.2).

Table I: Salt Dependence of the Kinetic Parameters of Helix Dissociation

	TH3 3		TH3 4	
[Na^+] (M)	E_a (kJ mol^{-1})	k_d (s^{-1}) at 25 °C	E_a (kJ mol^{-1})	k_d (s^{-1}) at 25 °C
0.013	171 ± 8	51 ± 2	209 ± 17	46 ± 3
0.07	168 ± 5	39 ± 1	170 ± 7	27 ± 2
0.10	188 ± 4	34 ± 1	197 ± 3	26 ± 1
0.19	167 ± 8	28 ± 3	170 ± 6	22 ± 2
0.25	184 ± 4	12 ± 1	198 ± 8	12 ± 2

the results of such an analysis for the innermost imino resonance, TH3 4.

Since all three imino resonances broaden and disappear as a group and give similar values for E_a and k_{ex}, it is likely that they are monitoring the same kinetic event. As discussed below, this event corresponds most reasonably to the dissociation of the oligomeric duplex into single strands (pathway II).

In Table I, we show the kinetic parameters of duplex dissociation obtained from salt-dependent Arrhenius plots for the

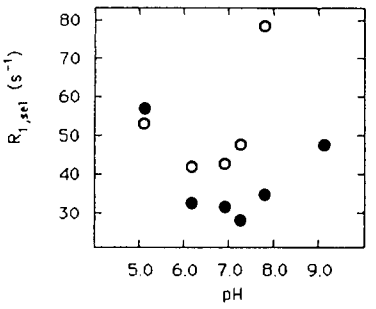

FIGURE 8: pH dependence of $R_{1,sel}$ at 25 °C for the internal imino protons of GGAATTCC for a sample containing 0.075 M Na^+, 11.5 mM GGAATTCC strand, and 1 mM EDTA. (○) TH3 3; (●) TH3 4.

two internal TH3 resonances. Again, similar E_a's and k_{ex}'s are obtained for the two resonances. E_a appears independent of the total sodium concentration, whereas a significant salt dependence is observed for k_{ex}(25 °C). In Figure 7, we show the results of our determinations of the salt dependence of k_{ex}(25 °C) over a range of DNA concentrations. Since all points fall on the same line [log k_{ex} = −0.57 (±0.1) log [Na^+] + 0.83 (±0.2)], there is no contribution to k_{ex} from the association reaction, and thus at low pH, $k_{ex} = k_d$. From the slope of the line, we determine that 0.57 ± 0.1 sodium ion is released upon the dissociation of the duplex.

pH and Base Catalyst Dependence of the Imino Proton Relaxation. Figure 8 shows the pH dependence of the selective T_1 relaxation of the TH3 imino protons. In qualitative agreement with the pH-dependent broadening observed in Figure 3, $R_{1,sel}$ for TH3 3 shows a very steep dependence on pH above pH 7, whereas $R_{1,sel}$ for TH3 4 is roughly independent of pH over the range of 6–8 pH units and begins to increase only thereafter. Between pH 6 and 7, the $R_{1,sel}$ of TH3 3 is also pH independent and similar in magnitude to that of TH3 4, though consistently somewhat higher. The slight increase in magnitude at low pH is reproducible. At even lower pH (pH 4 or less), additional exchangeable peaks appear at around 11 ppm (data not shown), probably resulting from partial base pairing of protonated bases. It is possible that the increase in $R_{1,sel}$ as the pH is lowered may result from an exchange between the low-pH form and the Watson–Crick base-paired form observed over the pH range of the present study.

As can be seen in Figure 9, Tris is also effective at increasing $R_{1,sel}$. In this figure is shown the effect of titrating with Tris on the $R_{1,sel}$ of TH3 4 at three different sodium ion concentrations. As outlined under Theory, data are plotted as $\tau_{ex} = (R_{1,sel} - R_{1,M} - k_d)^{-1}$ vs [base]$^{-1}$, where [base] is the concentration of Tris in the deprotonated form. k_d is determined at each point in the titration using log k_d = −0.57 log [M^+] + 0.83, where [M^+] is the total concentration of monovalent cation (sodium ion plus protonated Tris). Within experimental uncertainty, all of the experimental data fall on the same line, and thus, τ_0 and B_{eq} are salt independent. From the slope and intercept of the line at 0.42 M Na^+, we determine values for τ_0 of 9.5 (±4) ms and for B_{eq} of 93 (±30) mM at 25 °C. Using eq 7, we then determine $k_{cl}/\alpha = 2.0 \times 10^7$ s^{-1} under these conditions. For the remaining imino protons, we are not able to determine τ_0 or B_{eq} accurately, though both quantities appear to decrease upon moving toward the ends of the duplex. Figure 10 shows the temperature dependence of $R_{1,sel}$ for TH3 4 under conditions of excess Tris, so that τ_{ex} is nearly equal to τ_0(τ_{ex} = 16 ms at 25 °C under these conditions). From this curve, we determine that E_a is equal to 116 (±4) kJ/mol for the small-scale opening event that dominates the relaxation

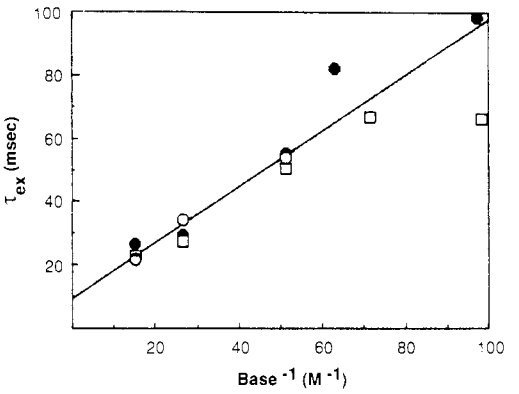

FIGURE 9: Dependence of $\tau_{ex} = (R_{1,sel} - R_{1,M} - k_d)^{-1}$ on the inverse of the concentration of Tris base at 25 °C, pH 7.8. $R_{1,M}$ was taken to be 2.0 s^{-1}, based on the extrapolation of low-temperature data as shown in Figure 6 (dashed line). The concentration of Tris base was calculated from the total Tris concentration using a pK_a of 8.14 for the Tris protonation equilibrium. k_d was calculated for each point by using log k_d = −0.57 (±0.1) log [M^+] + 0.83 (±0.2), where [M^+] is the concentration of sodium ion plus protonated Tris. (●) Octamer strand concentration = 0.83 mM, [Na^+] = 0.42 M; (○) strand concentration = 5.1 mM, [Na^+] = 0.30 M; (□) strand concentration = 11.5 mM, [Na^+] = 0.075 M. The solid line represents the best linear least-squares fit of the data at 0.42 M Na^+. From the intercept and slope of this line, we obtain B_{eq} = 0.093 ± 0.03 M and τ_0 = 9.5 ± 4 ms. Applying eq 7 gives $k_{cl}/\alpha = 2.0 \times 10^7$ s^{-1}.

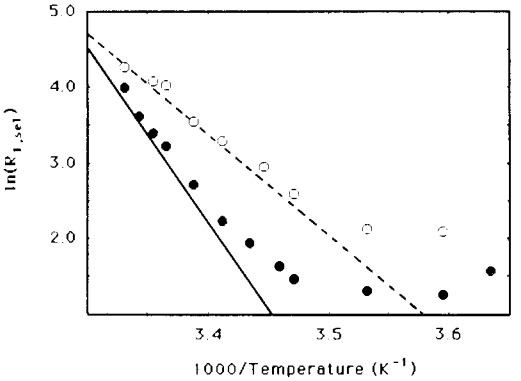

FIGURE 10: Arrhenius plot showing the temperature dependence of the TH3 4 imino proton resonance for samples containing (●) no added Tris, 0.1 M Na^+, 14.4 mM GGAATTCC strand, and 1 mM EDTA, pH 6.5; (○) 0.12 M Tris, 0.07 M Na^+, 10.1 mM GGAATTCC strand, and 1 mM EDTA, pH 7.8. The solid and dashed lines represent the exchange contribution to the relaxation for the sample in the absence and presence of added Tris, respectively. The exchange contribution was determined as outlined in the text and illustrated in Figure 6. From the slopes of these lines, we determine that E_a = 197 ± 3 kJ/mol in the absence of added Tris, whereas for the sample containing added Tris, E_a is decreased to 116 ± 4 kJ/mol.

under these conditions. Also shown in Figure 10 is the temperature dependence of $R_{1,sel}$ for TH3 4 in the absence of added Tris, from which an activation energy of 197 (±3) kJ/mol is obtained. Thus, the addition of Tris lowers the activation energy by about 80 kJ/mol.

Spermidine Dependence of the Imino Proton Relaxation. As shown in Figure 11, under low-salt and low-pH conditions, substoichiometric amounts of spermidine dramatically decrease $R_{1,sel}$, demonstrating that spermidine strongly stabilizes the octamer duplex with respect to strand dissociation. At higher salt concentrations, this effect is overwhelmed by the salt-induced stabilization discussed above, even though less spermidine is probably bound under these conditions (Braunlin et al., 1982). Thus, we find that for a sample containing 0.2 M Na^+ and 2.4 mM oligomer, pH 6.5, $R_{1,sel}$ remains constant at 20 s^{-1} upon the addition of 3 mM spermidine. The activation energy for helix dissociation does not appear to be

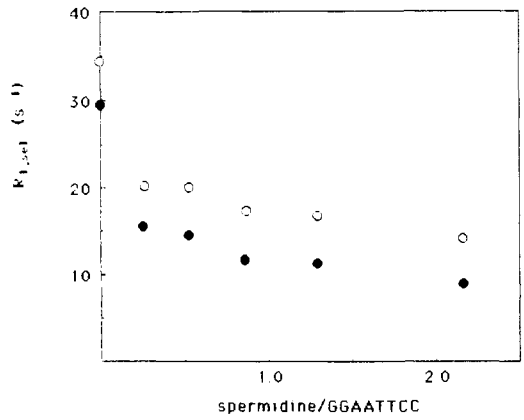

FIGURE 11: Effect of titration with spermidine on $R_{1,sel}$ for a sample at pH 6.3 containing 0.07 M Na^+, 7.7 mM GGAATTCC strand, 1 mM cacodylate, and 0.1 mM EDTA. (○) TH3 3 imino resonance; (●) TH3 4 imino resonance.

strongly affected by spermidine. Thus, for the sample of Figure 11, we obtain E_a = 170 (±5) kJ/mol and k_d = 27 (±2) s^{-1} at 25 °C for TH3 4 in the absence of added spermidine, whereas in the presence of 17 mM spermidine, pH 6.5, we obtain E_a = 225 (±20) kJ/mol and k_d = 5.3 (±4) s^{-1} at 25 °C.

As shown in Figure 12, as the pH is raised, spermidine acts as an extremely effective catalyst for imino proton exchange. From the limiting slopes and intercepts of the curves of Figure 12, we determine that τ_0 is roughly the same for Tris base and for divalent spermidine but that B_{eq} is about 10-fold smaller for spermidine. About half of this difference may be attributed to the difference in the pK_a's of Tris and spermidine. Thus, we find that k_{cl}/α is about 5 times greater for Tris than for spermidine. We also find that the value obtained for E_a for the small-scale opening event monitored at high Tris concentration is the same as that obtained under conditions of excess divalent spermidine. For the sample of Figure 12, containing 14 mM spermidine at pH 8.3, we obtain E_a = 130 (±7) kJ/mol and τ_{ex} = 16 ms at 25 °C.

Discussion

Exchange Kinetics of the Imino Resonances. As outlined in Figure 1, imino proton exchange of oligomeric DNA may occur through small-scale opening or following total dissociation of the duplex into single strands. Under conditions of low pH and low added catalyst, exchange of the internal imino resonances occurs primarily via duplex dissociation (pathway II), based on the following evidence:

(1) The three innermost imino resonances broaden and disappear as a group as the temperature is raised. Were pathway I contributing significantly to the relaxation, we would expect sequential broadening from the exterior of the helix toward the interior (Patel & Hilbers, 1975).

(2) The values obtained for k_{ex} and E_a for imino proton exchange are nearly the same for all three internal imino resonances (Figure 6 and Table I), indicating again that they are monitoring the same kinetic process.

(3) No oligomer concentration dependence is found for k_{ex}, indicating no dependence on the association rate (Figure 7).

(4) The values found for E_a are comparable to those found for the dissociation of other octamer duplexes (Pörschke et al., 1973).

At higher pH, and as base catalyst is added, the imino proton exchange becomes increasingly dominated by the small-scale opening of one or a few base pairs (pathway I), as evidenced by the following:

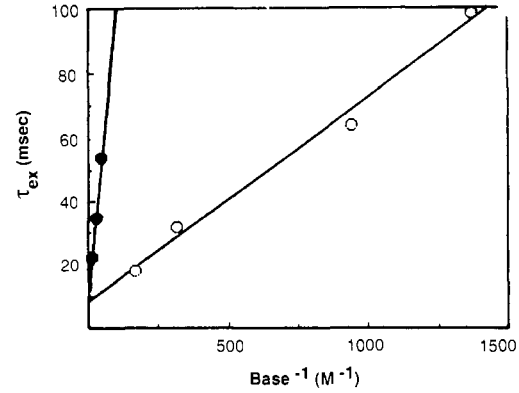

FIGURE 12: Dependence of $\tau_{ex} = (R_{1,sel} - R_{1,M} - k_d)^{-1}$ on the inverse of the concentration of base catalyst [Tris or diprotonated spermidine(2+)]. The open circles show the spermidine data over the course of a titration with NaOH of a sample containing 0.07 M Na^+, 7.7 mM GGAATTCC strand, 1 mM cacodylate, 14 mM spermidine, and 0.1 mM EDTA. The sample temperature was 25 °C, k_d was taken to be 5.6 s^{-1}, and $R_{1,M}$ was again taken to be 2.0 s^{-1}. The concentration of spermidine(2+) was calculated from the total spermidine concentration by using a pK_a value of 8.3 for the spermidine(3+) to spermidine(2+) equilibrium (Hedwig & Powell, 1973). The closed circles show for comparison the data of Figure 9 at 0.42 M Na^+ for a titration of GGAATTCC with Tris buffer at pH 7.8. The solid lines represent linear least-squares fits of the data. From the intercept and slope of the spermidine line, we obtain B_{eq} = 12.7 ± 4 mM and τ_0 = 5.5 ± 3 ms. k_{cl}/α is found to equal 4.0 × 10^6 s^{-1}. The corresponding values for the Tris data are, as given in Figure 9, B_{eq} = 0.093 ± 0.03 M, τ_0 = 9.5 ± 4 ms, and k_{cl}/α = 2.0 × 10^7 s^{-1}.

(1) As the pH is raised, resonances broaden sequentially from the exterior toward the interior of the helix.

(2) As the pH is raised, a sequential increase from the exterior toward the interior of the helix is also observed for $R_{1,sel}$.

(3) For high concentrations of added base catalyst, activation energies are obtained that are consistent with those that have been determined for small-scale opening reactions of double-helical nucleic acids. For example, Leroy et al. (1985) have determined E_a = 71 kJ/mol for the small-scale opening of poly(rA)·poly(rU), which compares well with the value of 116 kJ/mol that we obtain for the opening of the central A-T base pair of GGAATTCC. The opening rate constants obtained from extrapolations to infinite catalyst concentrations are also similar in magnitude to those found under similar conditions for the opening reactions of polymeric RNA (Leroy et al., 1985) and DNA (Plum and Bloomfield, unpublished results).

(4) No measurable salt or polyamine dependence is found for k_{ex} under conditions of high added catalyst. If exchange occurred through a large-scale dissociation event, a significant salt dependence might be expected.

To summarize, localized, uncorrelated opening events dominate the relaxation at high pH. Thus, large-scale "breathing" motions are not required for imino proton exchange. Nonetheless, as monitored by our low-pH measurements, opening of several base pairs at a time does occur and may lead to complete duplex dissociation of oligomeric helices.

Salt and Polyamine Dependences of the Exchange Kinetics. As we have demonstrated, both Na^+ and spermidine decrease the duplex dissociation rate of GGAATTCC. From the salt dependence shown in Figure 7, 0.6 ± 0.1 sodium ion is released in the transition state of helix dissociation. Since the activation energy for this process does not depend on the salt or spermidine concentrations, we conclude that the dissociation kinetics are entropically controlled by the release of bound counterions. This result is in contrast to the salt-*independent*

dissociation kinetics determined for oligomeric RNA containing a central GC core (Pörschke et al., 1973). We propose that for these RNA oligomers, the rate-limiting step involves the dissociation of the central GC core, for which little salt dependence is expected. In contrast, for d(GGAATTCC), dissociation seems to occur in a more all-or-none fashion, resulting in a larger salt dependence of k_d. We will discuss this point in more detail in another paper (Braunlin and Bloomfield, unpublished results), where we characterize the equilibria and kinetics of the association reaction. We note here, however, that the association kinetics of d(GGAATTCC) apparently have an even stronger salt dependence than do the dissociation kinetics ($\Delta \log k_a/\Delta \log [Na^+] = 1.6 \pm 0.3$).

Leroy et al. (1985) have examined the effectiveness of different catalysts at enhancing imino proton exchange of polyribonucleotides. These workers found Tris to be a highly effective base catalyst compared to other catalysts with lower pK_a's. Interestingly, although under the conditions of our experiments spermidine and Tris have comparable pK_a's, spermidine is an order of magnitude more effective than Tris at promoting imino proton exchange from the open state. The most straightforward explanation of this observation is that, due to its higher charge, spermidine is more highly concentrated near the DNA and thus has a greater opportunity to interact with the open state. Interestingly, within our experimental uncertainty, neither spermidine nor monovalent cation appears to significantly affect the rate of small-scale opening. This remark must, however, be qualified since the addition of Tris under the conditions of Figure 9 does increase the ionic strength of our solution, so that we have in fact only been able to determine τ_0 under relatively high ionic strength conditions.

Conclusions

From the results reported here, it is clear that solution conditions can profoundly influence the imino proton exchange results obtained for oligomeric DNA. By appropriately varying the pH and base catalyst concentrations, it is possible to select for conditions where exchange provides a monitor of helix dissociation at the one extreme and of small-scale openings of the duplex at the other. Our results clearly illustrate the importance of considering both types of opening events when attempting to understand the dynamics of DNA base-pairing reactions.

Under conditions at low pH and low added base catalyst, we have determined that the helix dissociation kinetics are limited by a transition involving the release of bound counterions. Spermidine is found to be particularly effective at diminishing the helix dissociation rate.

Under conditions of high added base catalyst, we have characterized small-scale opening events that occur on a time scale faster than the helix dissociation rate. Although diprotonated spermidine acts as an extremely effective catalyst of imino proton exchange, no dramatic effect of either spermidine or salt could be found on the local base-pair lifetime, a quantity which is found to equal 9.5 (±4) ms at 25 °C.

Acknowledgments

We thank Professor James Howard for use of the automated DNA synthesizer and Dr. David Ikeda for performing the oligonucleotide syntheses.

References

Behe, M., & Felsenfeld, G. (1981) *Proc. Natl. Acad. Sci. U.S.A. 78*, 1619.

Bendel, P. (1987) *Biopolymers 26*, 573.

Bloomfield, V. A., & Wilson, R. W. (1981) in *Polyamines in Biology and Medicine* (Morris, D. R., & Marton, L. J., Eds.) p 183, Marcel Dekker, New York.

Braunlin, W. H., Strick, T. J., & Record, M. T., Jr. (1982) *Biopolymers 21*, 1301.

Breslauer, K. J., & Bina-Stein, M. (1977) *Biophys. Chem. 7*, 211.

Broido, M. S., Zon, G., & James, T. L. (1984) *Biochem. Biophys. Res. Commun. 119*, 663.

Broido, M. S., James, T. L., Zon, G., & Keepers, J. W. (1985) *Eur. J. Biochem. 150*, 117.

Connolly, B. A., & Eckstein, F. (1984) *Biochemistry 23*, 5523.

Crothers, D. M., Cole, P. E., Hilbers, C. W., & Shulman, R. G. (1974) *J. Mol. Biol. 87*, 63.

Dickerson, R. F., & Drew, H. R. (1981) *J. Mol. Biol. 149*, 761.

Eigen, M. (1964) *Angew. Chem., Int. Ed. Engl. 3*, 1.

Good, N. E., Winget, G. D., Winter, W., Connolly, T. N., Izawa, S., & Singh, R. M. M. (1966) *Biochemistry 5*, 467.

Gosule, L. C., & Schellman, J. A. (1976) *Nature (London) 259*, 333.

Grable, J., Frederick, C. A., Samudzi, C., Jen-Jacobson, L., Lesser, D., Greene, P., Boyer, H. W., Itakura, K., & Rosenberg, J. M. (1984) *J. Biomol. Struct. Dyn. 1*, 1149.

Hartmann, B., Leng, M., & Ramstein, J. (1986) *Biochemistry 25*, 3073.

Hedwig, G. R., & Powell, H. K. J. (1973) *J. Chem. Soc., Dalton Trans.*, 793.

Johnston, P. D., & Redfield, A. G. (1981) *Biochemistry 20*, 3996.

Kearns, D. R. (1985) *CRC Crit. Rev. Biochem. 15*, 237.

Leroy, J.-L., Broseta, D., & Guéron, M. (1985) *J. Mol. Biol. 184*, 165.

Manning, G. S. (1976) *Biopolymers 15*, 1333.

Narang, S. A., Hsiung, H. M., & Brosseau, R. (1979) *Methods Enzymol. 68*, 90.

Narang, S. A., Brosseau, R., Hsiung, H. M., & Michniewicz, J. J. (1980) *Methods Enzymol. 65*, 610.

Nelson, J. W., & Tinoco, I., Jr. (1982) *Biochemistry 21*, 5289.

Ott, J., & Eckstein, F. (1985) *Biochemistry 24*, 2530.

Pardi, A., & Tinoco, I., Jr. (1982) *Biochemistry 21*, 4686.

Patel, D. J., & Hilbers, C. W. (1975) *Biochemistry 12*, 2651.

Patel, D. J., & Canuel, L. L. (1979) *Eur. J. Biochem. 96*, 267.

Patel, D. J., Kozlowski, S. A., Marky, L. A., Broka, C., Rice, J. A., Itakura, K., & Breslauer, K. J. (1982a) *Biochemistry 21*, 428.

Patel, D. J., Kozlowski, S. A., Marky, L. A., Rice, J. A., Broka, C., Itakura, K., & Breslauer, K. J. (1982b) *Biochemistry 21*, 451.

Patel, D. J., Pardi, A., & Itakura, K. (1982c) *Science (Washington, D.C.) 216*, 581.

Pörschke, D., Uhlenbeck, O. C., & Martin, F. H. (1973) *Biopolymers 12*, 1313.

Quigley, G. J., Teeter, M. M., & Rich, A. (1978) *Proc. Natl. Acad. Sci. U.S.A. 75*, 64.

Record, M. T., Jr., Mazur, S. J., Melançon, P., Roe, J.-H., Shaner, S. L., & Unger, L. (1981) *Annu. Rev. Biochem. 50*, 997.

Redfield, A. G., Kunz, S. D., & Ralph, E. K. (1975) *J. Magn. Reson. 19*, 114.

Rich, A., Mordheim, A., & Wang, A. H.-J. (1984) *Annu. Rev. Biochem. 53*, 791.

Sarma, R. H., Wagner, B. J., & Mitra, C. K. (1981) in *Proceedings of the Second SUNYA Conversation in the*

Discipline Biomolecular Stereodynamics (Sarma, R. H., Ed.) Vol. I, pp 89–98, Adenine, New York.
Ts'o, P. O. P. (1974) in *Basic Principles of Nucleic Acid Chemistry* (Ts'o, P. O. P., Ed.) Vol. 1, p 466, Academic, New York.
Valcour, A. A., & Woodworth, R. C. (1986) *J. Magn. Reson. 66*, 536.
Weast, R. C., Ed. (1983) *CRC Handbook of Chemistry and Physics*, p F-40, Chemical Rubber Publishing Co., Cleveland, OH.
Wemmer, D. E., & Reid, B. R. (1985) *Annu. Rev. Phys. Chem. 36*, 105.
Wilson, R. W., & Bloomfield, V. A. (1979) *Biochemistry 18*, 2192.

Coherence Transfer in Deoxyribose Sugars Produced by Isotropic Mixing: An Improved Intraresidue Assignment Strategy for the Two-Dimensional NMR Spectra of DNA†

Peter F. Flynn,* Agustin Kintanar, Brian R. Reid, and Gary Drobny
Department of Chemistry and Department of Biochemistry, University of Washington, Seattle, Washington 98195
Received June 16, 1987; Revised Manuscript Received October 5, 1987

ABSTRACT: Two-dimensional isotropic mixing spectroscopy has been used to confirm assignments of the deoxyribose sugar protons in the ^{1}H NMR spectrum of the DNA oligonucleotides d(CGCGTTTTCGCG) and [d(GCCGTGGCCACGGC)]$_2$. The broad-band decoupling sequence MLEV-16 was applied during the mixing period to induce isotropic coupling within the spin systems, resulting in net transfer of coherence throughout the coupled spin networks. Nearly all 1′, 2′, 2″, 3′, and 4′ protons of a given nucleotide could be identified on the basis of through-bond scalar connectivities. In addition, in the hairpin, a number of connectivities to 5′/5″ protons were found. The dependence of cross-peak intensity on the length of radio-frequency irradiation for several different coherence transfer orders is presented, and implications for optimization are discussed.

Two-dimensional NMR spectroscopy (2D NMR)[1] has become a valuable tool for investigating the solution structure of biological macromolecules. The success of the 2D NMR method lies in its ability to systematically assign the ^{1}H resonances in relatively complicated NMR spectra to specific atoms in the biopolymer; the high-resolution ^{1}H NMR spectra of DNA and proteins are typically too complex to be assigned by ordinary one-dimensional NMR methods. In addition to the resonance assignments, the 2D NMR method can yield interproton distances from the nuclear Overhauser effect (NOE) intensities, and such distances have been used to obtain qualitative solution structures in DNA and proteins [for a review, see Wemmer and Reid (1985)]. Trial structures based on model building or distance geometry matrix embedding methods can be generated and refined on the basis of these NOE-derived interproton distances to yield more quantitative three-dimensional structures (Kaptein et al., 1985; Havel & Wüthrich, 1985; Braun & Gō, 1986; Hare & Reid, 1986; Hare et al., 1986a,b).

The assignment strategy for synthetic right-handed double-helical DNA oligonucleotides has been developed by a number of independent laboratories (Feigon et al., 1983; Hare et al., 1983; Scheek et al., 1983). It consists of first identifying the resonances within a given deoxyribose sugar by their scalar coupling to adjacent vicinal protons with two-dimensional correlated spectroscopy (COSY). The isolated scalar-coupled spin systems are then associated with a particular nucleotide residue by establishment of sequential interresidue connectivities with two-dimensional nuclear Overhauser effect spectroscopy (NOESY). In practice, it is often difficult to delineate the entire coupled spin system of an isolated sugar ring with the COSY experiment because the 3′, 4′, 5′, and 5″ proton resonances fall within a narrow chemical shift range; thus, their cross-peaks fall close to the diagonal and are often difficult to resolve.

Relayed coherence transfer spectroscopy (RELAY) has been used in conjunction with the COSY experiment to extend the spin connectivity network to include 1′H–3′H and 2′H–4′H connectivities (Chazin et al., 1986; Hare & Reid, 1986). The RELAY experiment generates coherence between two protons that are not directly J coupled but are each coupled to a common spin. In practice, one can optimize the RELAY experiment to obtain all of the 1′H to 3′H cross-peaks, but it has proven to be much more difficult to observe all of the 2′H to 4′H cross-peaks with this experiment. The 2″H to 4′H cross-peaks in DNA are generally not observed by this method because of the extremely weak J coupling between 2″H and 3′H in the sugar conformations near the C2′-endo range of puckering. Cross-peaks between the 3′ and the 5′/5″ protons are likewise rarely seen, presumably because of weak scalar coupling between 3′H and 4′H or between 4′H and the 5′H, or both. Chazin and co-workers (Chazin et al., 1986) have been able to directly determine the 3′H–4′H connectivities by using a double-quantum (2Q) experiment (Braunschweiler et al., 1983). Although it should be possible in principle to establish the 1′H to 4′H and 2′H to 5′H/5″H scalar con-

† This work was supported by National Institutes of Health Grant GM-32681-03 to B.R.R. and to G.D.

[1] Abbreviations: 2D NMR, two-dimensional nuclear magnetic resonance; 2Q, double quantum; COSY, two-dimensional autocorrelated spectroscopy; RELAY, two-dimensional relayed coherence transfer spectroscopy; NOE, nuclear Overhauser effect; NOESY, two-dimensional nuclear Overhauser effect spectroscopy.

0006-2960/88/0427-1191$01.50/0